Thermal creep of shear tab connection assemblies under transient-state temperatures of fire

Karim Al Khatib and Elie Hantouche
Faculty of Engineering and Architecture, American University of Beirut, Beirut, Lebanon, and

Mohammed Ali Morovat
University of Texas, Austin, Texas, USA

Received 9 July 2018
Revised 18 September 2018
Accepted 10 December 2018

Abstract

Purpose – This study aims to investigate the thermal creep behavior of steel frame assemblies with shear tab connections subjected to transient-state fire temperatures. Different key parameters are investigated to study their effect on the global response of the steel frames in fire.

Design/methodology/approach – Finite element (FE) models of connection assemblies are first analyzed using Abaqus under transient-state temperature conditions and validated against experimental work available in the literature. Upon acquiring the validated conditions, parametric studies are carried out to study the effect of key geometric and heating parameters on the overall response of the frame assembly to fire temperatures. Thermal creep material is also incorporated in the analyses through a user-defined subroutine, and a comparison between including and excluding creep material is illustrated to show the effect of thermal creep on the structural behavior.

Findings – The results reported herein indicate that having a rigid column increases the thermal-induced axial forces, thus increasing the development of thermal creep strains. Slow heating rates can cause axial stress relaxation in the restrained beam and increase the mid-span deflection and consequently the development of beam catenary action. The results also show that reaching higher initial cooling temperatures and having longer cooling phase durations result in more tensile forces at the end of the cooling phase.

Originality/value – Previous studies were limited to isolated steel connections under steady-state conditions. This study investigates the creep behavior of shear tab connection assemblies under transient-state conditions of fire when creep effects are explicitly considered. This can provide a rational and realistic assessment of the steel behavior in fire events.

Keywords Finite element modeling, Shear tab connection assemblies, Steel creep, Thermally restrained beams, Structural-fire

Paper type Research paper

1. Introduction

Structural-fire safety is an important consideration when designing high-rise steel structures. Steel material is well known for having a good performance by means of high strength, stiffness and ductility at ambient temperatures. However, in fire, steel material experiences severe strength and stiffness degradation in addition to the induced thermal loads caused by restrained thermal expansion and geometrical nonlinearities.

The authors gratefully acknowledge the financial support provided by the American University of Beirut Research Board under grant No.103604-24705.

Journal of Structural Fire Engineering
Vol. 10 No. 3, 2019
pp. 297-316

2040-2317
DOI 10.1108/JSFE-07-2018-0016

Steel connections play an important role in providing structural stability and integrity. Failure of one or more of these connections can lead to total structural collapse. Simple (shear) steel beam-column connections are extensively used in steel structures due to the ease of construction and fabrication. They are usually considered, by designers, as ideally pinned joints that allow relative rotation and completely prevent the transition of bending moment between structural members. However, in fire events, these connections exhibit a complex response, and studying their behavior under fire conditions is of great importance. A commonly used simple steel beam-column connection in the US is the shear tab connection. It is known that this type of connection has a high rotational capacity and provides high ductility mainly due to the elongation of holes in bearing (Wald *et al.*, 2006). Ductility of steel connections is a very important factor for the survival of steel beams in fire events by contributing to the redistribution of forces between supporting regions. Redistribution of forces can delay or prevent the beam failure and result in a ductile performance, which is more favorable in fire events than a brittle failure (Pakala and Kodur, 2016).

Extensive experimental and numerical studies were carried out to study the performance of isolated steel connections at elevated temperatures (Yu *et al.*, 2009a, 2009b; Hu and Engelhardt, 2014; Hantouche and Sleiman, 2015). In fire, however, the behavior of steel connections is highly controlled by the interaction with the connected members (beams and columns) and also with the neighboring unheated members. Therefore, designing steel connections to withstand different fire scenarios should consider interactions between members in structural frame systems rather than treating the connections as isolated structural elements.

To model the effect of temperature on mechanical properties of structural steel, fire design codes use the concept of retention factors that are solely dependent on the instant temperature of steel (Lie, 1992; Poh, 2001; EN 1995-1-2, 2005). Nonetheless, at elevated temperatures, steel behavior is greatly influenced by the development of time-dependent strains, known as thermal creep strains. Thermal creep strains are time-dependent inelastic (plastic) strains that can cause permanent structural deformations. When steel temperature exceeds around one-third of its melting point accompanied with applied stresses, creep effect becomes significant and can greatly change the overall structural behavior (Torić *et al.*, 2013).

It was not until recently that the time-dependent behavior of steel structures in fire received more attention from researchers (Kodur and Dwaikat, 2010; Torić *et al.*, 2013; Morovat *et al.*, 2014; Morovat *et al.*, 2018) who reported that time is an important factor that should be considered in analyses of steel structures in fire. Although stress-strain-temperature curves in design codes (EN 1995-1-2, 2005) consider creep strains implicitly, recent studies showed that explicit consideration of creep is more appropriate and can result in a more accurate representation of the real case (Kodur and Dwaikat, 2010).

The assessment of the fire resistance of steel connections should be carried out based on its performance in full-scale systems or the so-called performance-based design approach. Accurate predictions of a performance-based design approach depend on realistic representation of both loading conditions and material behavior. For that reason, it is essential to include thermal creep effect, which is significant at high temperatures, when analyzing the structural fire resistance. Several experimental and numerical studies were conducted to further understand the time-dependent response of steel structures when subjected to fire temperatures. A methodology was proposed to study the creep buckling of columns (Morovat *et al.*, 2014). It was shown that the column buckling does not depend only on the slenderness and the steel temperature, but also on the duration at which the load is applied. Explicit consideration of creep allows quantifying the time effect on the behavior of steel structures at high temperatures. That was clearly manifested in the investigation of the

WTC building collapse on September 11, 2001. The importance of thermal creep of steel was recognized and included in all the finite element (FE) simulations (Luecke *et al.*, 2005).

In this study, the thermal creep effect is introduced into the FE models in Abaqus, through a newly developed user-defined subroutine. The development of the subroutine is based on Fields and Fields (1989) constitutive creep model and follows available Abaqus documentations (Abaqus Ver. 6.14 Documentation, 2014). First, FE models of the steel frames with shear tab connections are developed. The FE models follow the same geometric and material properties reported in Wang *et al.* (2011) fire tests (Tests 1 and 6) performed at the University of Manchester. The results obtained from the FE models are validated against those obtained from the experiment. Then, FE models of the connection assembly are further generated and used to conduct an extensive parametric study of key parameters that affect the time-dependent behavior of the system during the heating and cooling phases of fire. These parameters are heating rate, column size, cooling duration, initial cooling temperature, beam geometry and shear tab location. The results obtained from the FE models are compared, discussed and analyzed to give more insights on the impact of thermal creep on steel frames with shear tab connections.

2. Thermal creep of structural steel

Previous models were developed to include the thermal creep effect in FE models, some of which accounted for creep explicitly by using predefined equations in user-defined subroutines or implicitly by including its effect in the steel temperature-stress-strain curves.

2.1 Creep models in literature

Explicit inclusion of the creep effects in FE packages, such as Abaqus and Ansys, requires well-defined constitutive creep models capable of predicting creep strain development under different conditions of temperatures and stresses. These models can be established based on material creep tests conducted under stationary or transient conditions (Harmathy, 1967; Fields and Fields, 1989; Matar *et al.*, 2014; Wang *et al.*, 2016). The resulting creep equations describe the creep behavior by an equivalent uniaxial behavior. In most cases, creep curves can be divided into three stages with respect to time, as shown in Figure 1. Once the load is applied, a primary stage takes place that is described by creep rates that decrease with time. The secondary stage is associated with a slow but steady rate through time. Finally, prior to failure, creep rate increases exponentially until the specimen ruptures; this stage is denoted

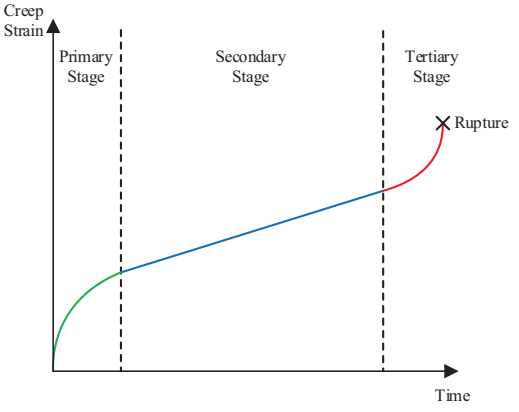

Figure 1.
Typical creep curve of structural steel

by the tertiary stage. The tertiary creep stage is usually not recognized in creep models since it implies impending failure (Dwaikat and Kodur, 2009). Therefore, only the primary and secondary stages of creep are included in the structural fire analyses.

Harmathy (1967) developed a model that predicts the time-dependent strains for ASTM A36 steel under elevated temperatures (up to 700°C). Much existing work used Harmathy (1967) model to include the creep effect (Tan *et al.*, 2002; Huang and Tan, 2004; Torić *et al.*, 2013). However, this model is limited to cases where stress is assumed constant. To address this shortcoming, many empirical models (Williams-leir, 1983; Fields and Fields, 1989; Kodur and Dwaikat, 2010) are developed based on experimental tests. These models are developed through fitting experimental data into creep equations that can take different forms (power law, exponential law, etc.) depending on the material behavior. For example, Fields and Fields (1989) used tensile and creep tests available in the literature to study the deformation mechanism of ASTM A36 steel (equivalent to S275 steel). The total strain was divided into different components where creep strain was considered as an explicit/independent component.

2.2 Development of creep strains

The total strain is the summation of both thermal and mechanical strains that can be divided into time-dependent and time-independent strains. When considering creep strain as an independent component, the total strain can be written as follows:

$$\varepsilon_T = \varepsilon_e(\sigma, T) + \varepsilon_p(\sigma, T) + \varepsilon_{th}(T) + \varepsilon_c(t, \sigma, T) \tag{1}$$

where ε_T is the total strain, ε_e is the elastic time-independent strain, ε_p is the plastic time-independent strain, ε_{th} is the free thermal strain and ε_c is the creep (plastic time-dependent) strain. The two components ε_e and ε_p are dependent on the instant temperature (T) and stress (σ), ε_{th} is dependent on the temperature, and ε_c is time (t)-, stress- and temperature-dependent.

An empirical creep equation was proposed by Fields and Fields (1989) in the form of power law (Norton–Bailey) equation. This model is considered one of the most commonly used creep models in structural-fire engineering applications (Luecke *et al.*, 2005; Morovat *et al.*, 2014). It is developed for the ASTM A36 steel and can predict the creep in temperatures ranging from 350°C to 600°C under various stresses for creep strains up to 6 per cent. As discussed before, this model includes only the primary and secondary stages of creep (Figure 2). The equation is as follows:

$$\varepsilon_c = f(t, \sigma, T) = At^B\sigma^C \tag{2}$$

where the coefficients A, B and C are temperature-dependent material properties (Fields and Fields, 1989). Note that this equation incorporates the three factors (time, stress and temperature) affecting the development of creep strain. The creep strain rate, $\dot{\varepsilon}_c$, with respect to time is as follows:

$$\dot{\varepsilon}_c = f(t, \sigma, T) = ABt^{B-1}\sigma^C \tag{3}$$

The form of equation (3) is called time hardening formulation, where creep strain rate is in the function of time. However, it was shown by many researchers (Kodur and Dwaikat, 2010) that the strain hardening formulation, where the strain rate is in the function of creep

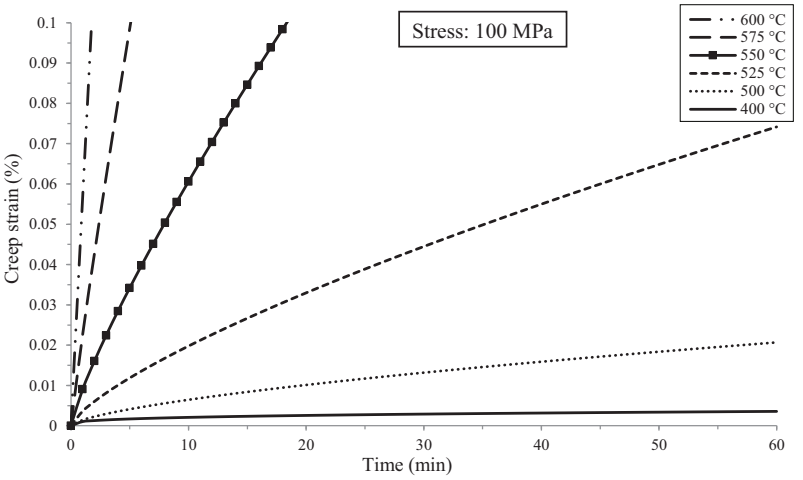

Figure 2.
Fields and Fields creep model of structural steel (1989)

strain history, can yield better and more accurate results especially for transient cases, thus equation (3) can be transformed as follows:

$$\dot{\varepsilon}_c = f(\varepsilon_c, \sigma, T) = A^{\frac{1}{B}} B \varepsilon_c^{\frac{B-1}{B}} \sigma^{\frac{C}{B}} \tag{4}$$

In fire events, steel structures are subjected to strongly variable conditions which make the analytical solution very complex, thus resorting to numerical solutions, such as the FE analysis. The total time is divided into small increments during each of which temperature and stress are assumed constant. At each increment, creep strain is calculated and introduced explicitly into the total strain [equation (1)] for each mesh element in the FE model. Within a given time step, Δt, the change in the creep strain, $\Delta\varepsilon_c$, in the explicit form can be represented as:

$$\Delta\varepsilon_c = \left(A^{\frac{1}{B}} B \varepsilon_c^{\frac{B-1}{B}} \sigma^{\frac{C}{B}}\right) \Delta t \tag{5}$$

Abaqus provides the means to include the creep strains into the FE models through the incorporation of a user-defined subroutine (CREEP). The subroutine is developed as per Abaqus documentation (Abaqus Ver. 6.14 Documentation, 2014) and based on Fields and Fields (1989) constitutive creep model, taking into account unit consistency. The developed subroutine can accommodate for transient-state conditions where temperature and/or stress are varying with time.

3. Shear tab connection assembly

Wang *et al.* (2011) conducted ten fire tests on five different types of steel connections with two different column sizes. Two of these fire tests were on shear tab connections (Tests 1 and 6). FE models of the two shear tab connection assemblies are developed in Abaqus to reproduce the same geometrical and material properties reported in the experiment. The assembly details are shown in Figure 3(a), and a summary of the component properties are presented in Table I. The results obtained from the FE models are then evaluated against the results from the corresponding experiment. A description of the structural components,

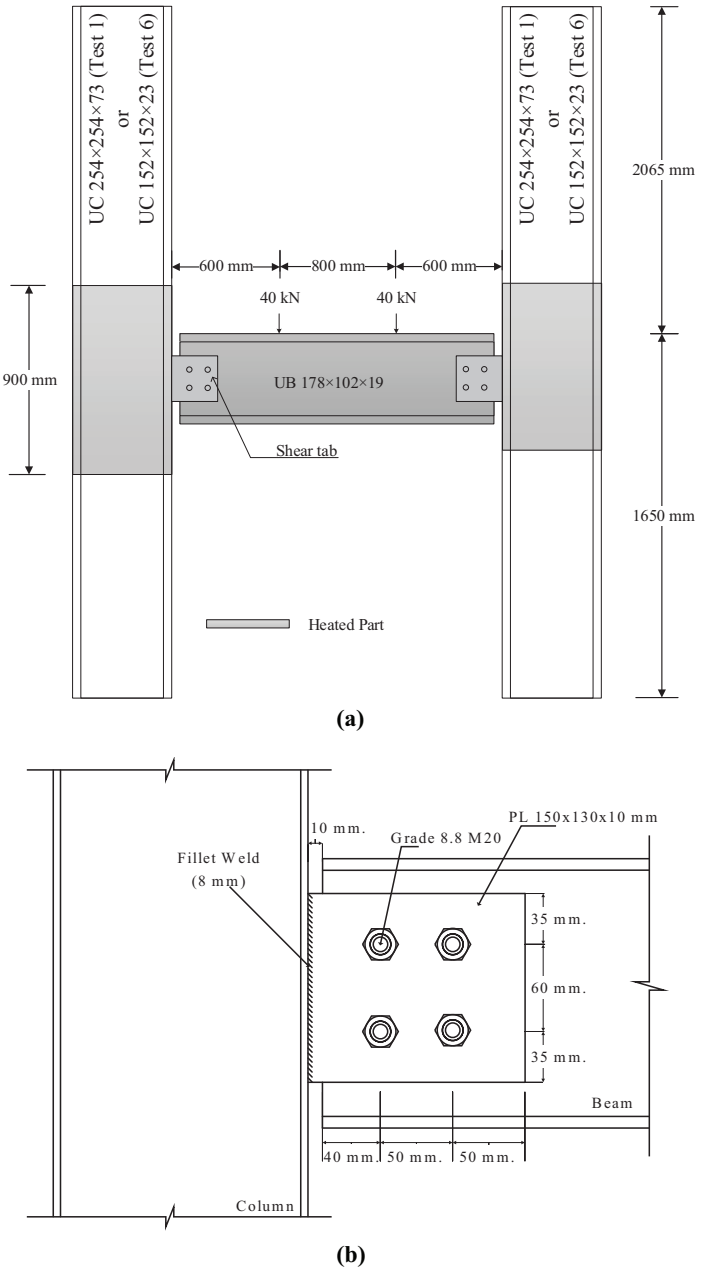

Figure 3.
Details on the fire tests assembly of Wang *et al.* (2011)

Notes: (a) Steel frame assembly; (b) shear tab connection

the analysis procedure conducted in the FE models, and the observations cited during the simulations are presented below.

3.1 Geometry of the structural components

The shear tab connection assembly used in the analyses consists of one steel plate 150 × 130 × 10 mm which connects a UB 178 × 102 × 19 beam to the column. Two different column sections are used: UC 254 × 254 × 73 for Test 1 and UC 152 × 152 × 23 for Test 6 (the same notation will be used for both cases hereafter). The plate is welded to the column while bolted to the beam. Four shear bolts of diameter 20 mm (M20) are used with bolt holes of diameter 22 mm (standard size holes). The details of the shear tab connection are shown in Figure 3(b).

3.1.1 Material properties. An idealized bilinear model is used for the steel materials to incorporate the isotropic hardening of steel with von Mises yielding criterion. The ambient material properties used for the structural parts in the FE models are in agreement with the material properties reported in the experiment. The shear tab plate and the beam are grade S275 steel, yet tensile coupon tests were performed, in the experiment, at ambient temperature and the average yield stress of the tensile coupons taken from the tested beams was found to be 345 N/mm^2. The UC 254 × 254 × 73 (Test 1) and UC 152 × 152 × 23 (Test 6) columns are of Grade S355 and S275 steel, respectively. The shear tab bolts and nuts are of Grade 8.8. For all the steel components, *Poisson's* ratio is taken as 0.3, and it is assumed to be temperature independent for steel.

Retention factors proposed by Lee *et al.* (2013) are used for the structural steel material, whereas the retention factors proposed by Hu *et al.* (2007) are used for the structural bolts. Due to fast heating (standard fire temperature-time curve) and the thermal gradient present in the structural components, creep material is not included in steel properties. Material fracture is not considered in the analyses.

3.1.2 Model discretization. All components of the assembly model in Abaqus are discretized using eight-node brick elements with reduced integration (C3D8-R). To account for the high stresses present in the connection region where the failure is likely to occur, a relatively finer mesh is used around the connection region. Moreover, to avoid stress concentration around the bolt holes, a mapped meshing technique is used to discretize bolts and their surrounding areas. The bolt heads, shanks and nuts are modeled as cylindrical volumes.

Surface-to-surface contact with a finite sliding coefficient is used to reproduce contact surfaces. A friction coefficient of 0.25 is used to model friction between the contact surfaces while allowing separation, sliding and rotation of the contact surfaces. Tie constraint is used to reproduce the fillet weld connecting the shear tab to the column.

Table I. Summary of the frame assembly components properties

Test No.	Frame components	Section/Dimension	Material grade
Test 1	Column	UC 254 × 254 × 73	S355
	Beam	UB178 × 102 × 19	S275
	Shear tab plate	PL 150 × 130 × 10	S275
	Bolts	Four M20 bolts	G8.8
Test 6	Column	UC 152 × 152 × 23	S275
	Beam	UB 178 × 102 × 19	S275
	Shear tab plate	PL 150 × 130 × 10	S275
	Bolts	Four M20 bolts	G8.8

3.1.3 Applied loads and boundary conditions. Two distinct loading steps are created, one for the pre-tensioning of the shear bolts and the other for applying the two concentrated loads of 40 kN each. Due to the perfect symmetry of structural assembly, half of the frame is modeled in Abaqus and symmetry is applied at the beam mid-span section to reduce computational time. It is assumed to have a constant force with symmetry applied at the mid-span.

To ensure stability between bolted elements, pre-tensioning of the bolts is done before applying the load to the beam. It is achieved by applying pressure load on the bolt ends with a force equivalent to the required pre-tensioning force. In the next step, a concentrated vertical force of 40 kN is applied to the steel beam monotonically. This load corresponds to a loading ratio of 0.5 of the plastic moment capacity of the beam section at ambient temperature. The concentrated force is represented by a pressure load distributed on a small area to avoid stress concentration. After that, the frame is heated while holding the applied load constant. Both column ends are horizontally restrained yet free to expand, due to heating, in the vertical direction. In the FE model, a horizontal restraint is assigned to the beam top flange to simulate the lateral restraint provided by the steel truss in the experiment.

3.1.4 Temperature profile. In addition to the steel truss connected to the beam top flange to impose horizontal restraint in the experiment, the beam top flange was also wrapped with isolating material to include the heat-sink effect of the concrete slab. The furnace size, as specified, was $3{,}000 \times 1{,}600 \times 900$ mm, hence part of the column was present inside the furnace and exposed to fire temperatures. Moreover, some difficulties were encountered in maintaining uniform distribution of temperature in the furnace and among the structural components of the frame throughout the test. All these factors imply that it is essential to assign different temperature profiles for the different structural components for the sake of including similar experimental conditions. Therefore, the FE model of the test specimen is divided into six regions, each having a uniform temperature distribution.

3.2 Discussion of the results

Comparison of the FE models' predictions with the experimental results is shown in Figure 4(a) and (b). The behavior of the steel frame is represented in terms of the induced beam axial force and the beam mid-span deflection. The case under study is transient-state heating of an axially restrained beam. The axial force is developed owing to the restrained expansion of the steel beam as shown in Figure 4(a). At the beginning of the heating phase, linear increase in the internal beam axial forces and a slight increase in the mid-span deflection can be seen, since no significant degradation in the material properties is present at low temperatures. In Test 1, at about 200°C, a sudden slip occurs between the shear tab plate and the connected beam web, as shown in Figure 5(a) and (b), which causes a loss in the stored thermal strain energy. Thus, releasing beam axial stresses. The slip between the plates is then followed by the bearing of the bolt shank [Figure 5(d)] with the bolt hole [Figure 5(b)]. No slip is observed in Test 6. In fact, Test 1 gave higher axial forces due to having stiffer columns than those of Test 6, but mid-span deflection is relatively similar in both cases. Afterward, a nonlinear increase in axial force and deflection is observed due to material strength and stiffness degradations as temperature increases. As mentioned before, the shear tab connection ductility is mainly due to the ovalization (elongation) of the bolt holes. This is also confirmed in the FE simulations [Figure 5(c)]. A comparison of the FE models and the corresponding experiment deformed shapes is illustrated in Figure 6. It can be seen that the FE simulations can predict closely the deformation response of the connection.

Numerical convergence issues are encountered before the start of the cooling (decay) phase. High stresses are observed at the shear tab plate near the vicinity of the weld which

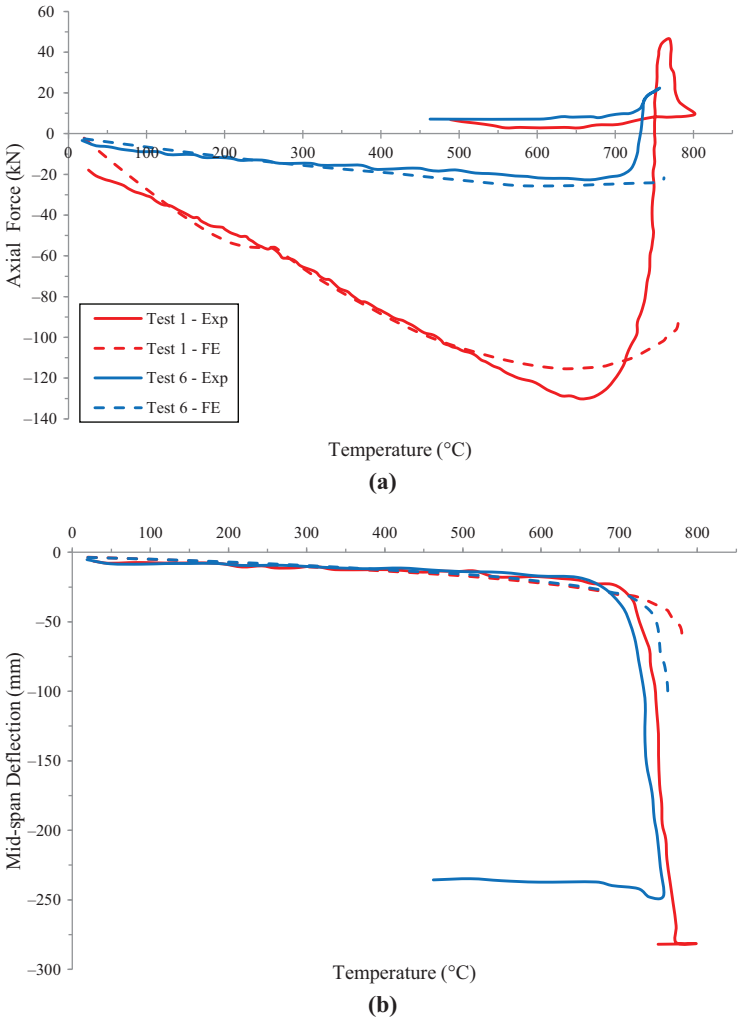

Notes: (a) Beam axial force; (b) beam mid-span deflection

Figure 4.
Comparison between the experimental and FE model results

indicates a potential weld fracture. The post-ultimate response of the structure cannot be reached in these simulations since the implicit (Abaqus/Standard) solver is used to run the simulations without the interference of any stabilizing options or the inclusion of material fracture properties.

4. Effect of thermal creep on the shear tab assembly response

The performance of the steel frame with a shear tab connection can be influenced by many factors. These factors can be the geometric configuration of the frame itself or even the fire scenario (temperature-time profile) which the frame is exposed to. Therefore, FE models of

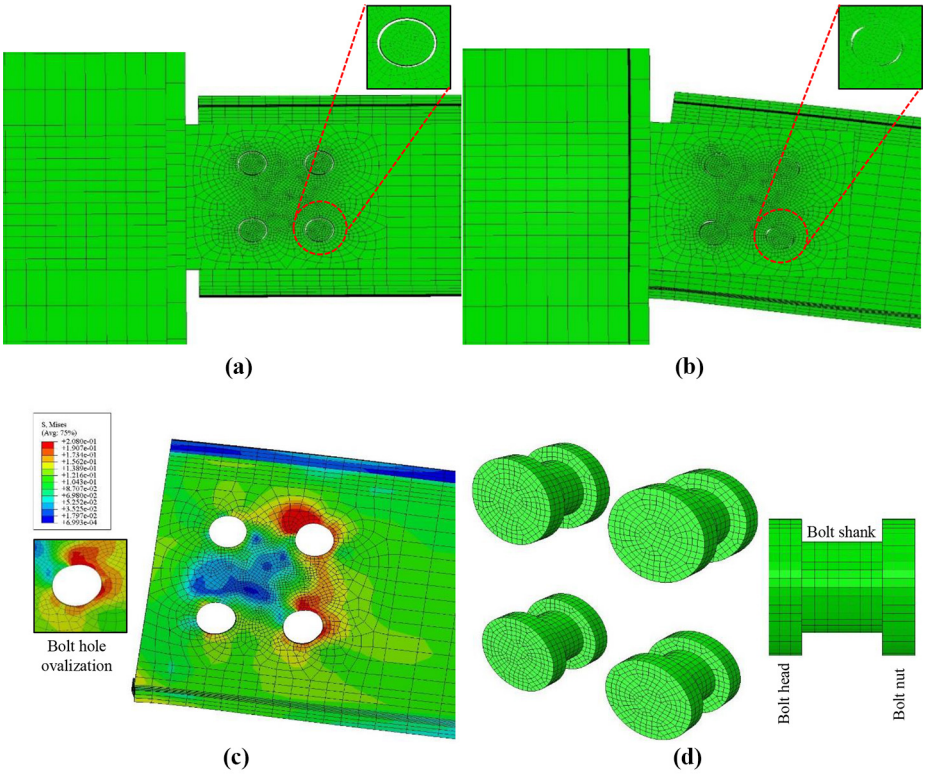

Figure 5.
Shear tab connection behavior

Notes: (a) Before bolt contact; (b) after bolt contact; (c) bolt hole ovalization (elongation); (d) modeling of shear bolts

the connection assembly are further generated and used to conduct an extensive parametric study of key parameters that affect the time-dependent behavior of the frame during the heating and cooling (decay) phases of fire. These parameters are heating rate, cooling duration, initial cooling temperature, column size, beam geometry and shear tab location. FE analysis has proven to be a reliable tool to predict the structural behavior and can reproduce complex geometrical and material nonlinearities. The results obtained from the FE models are compared, discussed and analyzed to investigate the impact of thermal creep on steel frames with shear tab connections.

4.1 Description of the connection assembly models

After obtaining the validated scenarios, an extensive parametric study is conducted with some modifications. Unlike the validated conditions, a uniform distribution of temperature is assigned to all the heated structural components for simplicity. In addition, due to the limitations imposed through the application of the creep model by Fields and Fields (1989), the maximum temperature of 600°C is considered. The developed user-defined subroutine is assigned to both the beam and the shear tab plate. Creep effect is not considered when modeling the bolts. Creep is also not incorporated in the steel column material. The

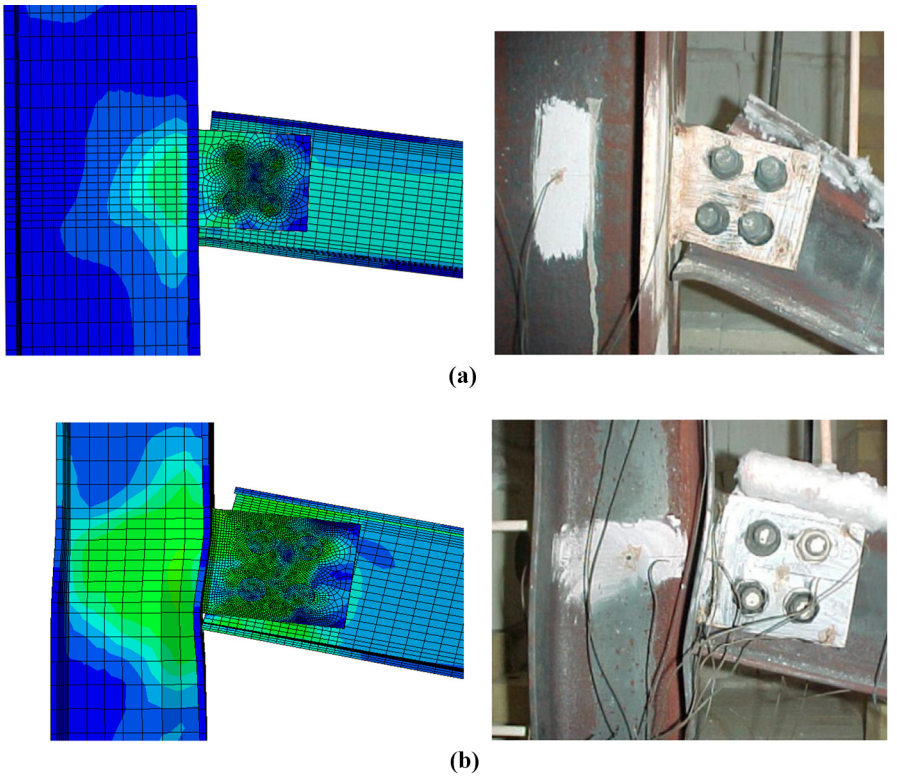

Notes: (a) Test 1; (b) Test 6

Figure 6.
Comparison between FE simulation and experimental (Wang *et al.*, 2011) deformed shapes after the fire test

developed user-defined subroutine is activated in the heating and cooling stages, both of which their type is changed to *VISCO*. The mesh element type used in the FE analysis (C3D8-R) is capable of incorporating creep strains. Moreover, in contrast to the conventional static (general) FE analysis, defining the time of the analysis step is important when introducing creep effect. During the analysis, the implicit integration scheme is always used for incorporation of creep strains development, as this method is unconditionally stable and can check for structural equilibrium and stability.

4.2 Parametric studies

4.2.1 Heating rate. The fact that creep strains are time-dependent strains entails that heating rate (temperature increase with time) is an important parameter that needs to be investigated. For the case of Test 1, three heating rates are chosen (5, 10 and 20°C/min) in addition to the case with no creep. Restricted to Fields and Fields (1989) limitations, the maximum temperature reached in the heating phase is 600°C. The results of the beam axial force and the beam mid-span deflection of Test 1 obtained from Abaqus are shown in Figure 7(a) and (b), respectively. At temperatures below 350°C, no effect of creep can be seen. This returns to the fact that the subroutine is developed based on Fields and Fields (1989) creep model which considers the temperature 350°C as a limiting temperature for creep

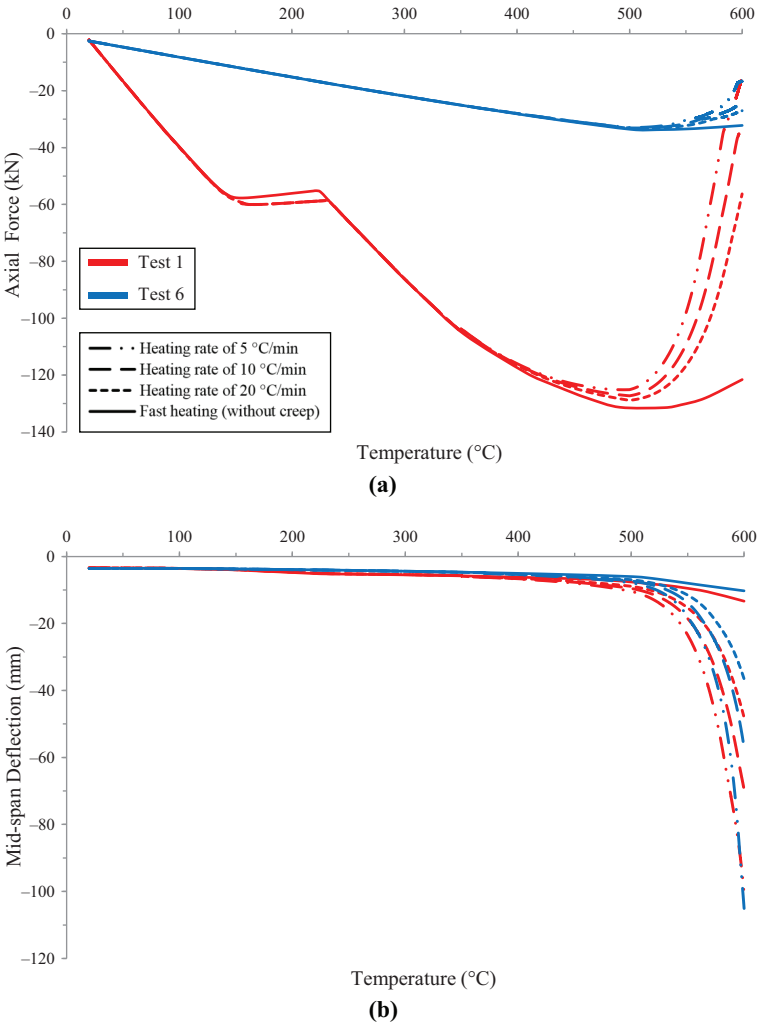

Figure 7.
Results obtained from Abaqus of different heating rates for Tests 1 and 6

Notes: (a) Beam axial force; (b) beam mid-span deflection

effect to initiate. Afterward, looking at the beam axial force in Figure 7(a), the phenomenon of stress relaxation can be clearly shown when introducing the creep effect into the FE models. This is attributed to having the case of a restrained beam subjected to temperature increase. Creep strains result in stress decrease in restrained systems with induced thermal axial stresses. In contrast, creep causes an increase in the beam mid-span deflection as shown in Figure 7(b) in response to the stresses of the bending moment caused by the constant applied load (40 kN). Moreover, with slow heating rates (e.g. 5°C/min) the creep effect is more significant: more beam mid-span deflection and more reduction in the axial force can be clearly seen. Nonetheless, the drop in the axial stresses is not entirely caused by

stress relaxation phenomenon but also by the geometrical and material nonlinearities, most notably the catenary action of the beam due to the increase in the beam deflection.

When the beam loses its flexural stiffness due to plastic strains or even creep effect and large deformations occur, the load is transferred through an alternative axial path that can maintain equilibrium and slow down beam deflection. The beam resistance mechanism changes from the flexural to the axial mechanism, well known as catenary action. This generates, if enough tying capacity exists in the connections, tensile forces in the beam which counteract the thermal compressive forces leading to a decrease in the axial stresses as shown in Figure 7(a). The catenary action is mainly dependent on the beam material and geometry, applied vertical load and the beam end axial stiffness restraint, represented by the column flexural stiffness.

Based on the used creep model, the creep strain rate increases exponentially as temperature increases, especially for temperatures higher than 500°C. That explains the fast drop in axial force and fast increase in the mid-span deflection at high temperatures (above 500°C). Furthermore, excessive elongation of the bolt holes is observed due to high stresses at the connection region.

4.2.2 Column size. The column size has a great impact on the response of the steel frame during fire. In addition to supporting gravity loads, columns also provide an axial restraint at the beam ends through its flexural stiffness. The column flexural stiffness is determined by its length, size (cross-section), boundary conditions and steel material properties. The two column sections of Tests 1 and 6 are used to represent different beam end restraint stiffnesses. FE models of the two column sizes are further developed with different heating rates to understand the effect of beam end restraint stiffness on the development of creep strains. The results of the beam axial force and the mid-span deflection of the two cases are presented in Figures 7(a) and (b), respectively. It is clearly evident that the column size can greatly influence the development of creep strains. The fact that the stress is a controlling factor of creep strain development [equation (2)], the high axial stresses in Test 1 expedite the development of creep strains, unlike Test 6. This is not the case for beam mid-span deflection where the results are relatively similar in both cases since they have the same applied load (40 kN) with a simple connection (shear tab connection). Nonetheless, Test 1 is seen to have slightly higher mid-span deflection when compared to Test 6. This is due to the P-Δ effect, where P is the induced axial force on the beam ends and Δ is the vertical deflection. The connection rotation shows a similar trend as the beam mid-span deflection as shown in Figure 8.

4.2.3 Cooling duration. In the decay phase of a fire, the temperature drops back to the ambient/room temperature (20°C). Note that the heating or cooling phases of fire do not directly contribute to the subroutine output since, as mentioned previously, the input temperature is the instant temperature and not the change (variation) in temperature (unlike thermal expansion) of steel at a given increment [equation (4)]. Moreover, the temperature does not control the sign (negative or positive increments) of the creep strain. Temperature is rather a factor of initiation of creep effect and one of the factors that control the rate of creep strain development.

Due to the lack of information about the material properties of steel (bolts, base material, etc.) after exposure to fire temperatures, it is assumed that all the assembly components regain their full strength and stiffness when cooled down to the ambient temperature (20°C). The subroutine is also incorporated in the cooling phase since cooling starts from high temperatures, where the creep effect is significant. Therefore, the response of the connection assembly in the cooling (decay) phase of fire is also considered through applying various cooling durations. Besides the case with no creep, three cooling durations are considered (5, 10 and 20 min). Figure 9 shows the beam axial force and mid-span deflection for different cooling durations after two heating cases: no creep and heating rate of 20°C/min. It can be

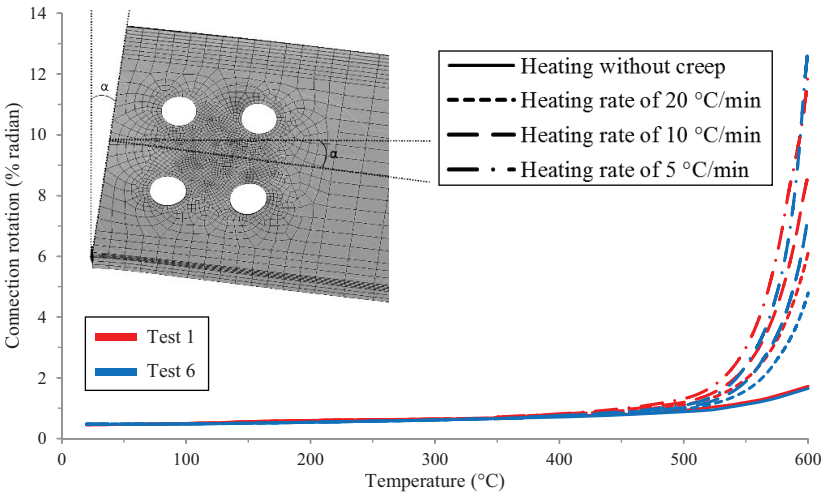

Figure 8.
Connection rotation results for different heating rates

seen that a slower heating rate produces large axial tensile forces at the end of the cooling phase. This can be attributed to the additional loss of the induced beam axial force, during the heating phase, due to the development of creep strains. For faster heating rates, the difference between the results of the four cooling durations can be clearly seen since the compression axial force at the end of the heating phase is larger, causing faster creep rate. When the tension force reaches almost the same magnitude (about 60 kN) at which the first slip occurred (during the heating phase), a reverse slip is observed during the cooling phase.

4.2.4 Initial cooling temperature. It was observed by many researchers that the failure of the connections occurs mostly during the decay phase of fire due to the generated tensile forces (Selamet and Garlock, 2010). Insufficient tying force capacity of steel connections can lead to failure of these connections. Depending on the fire scenario of which the frame is exposed to or whether the steel member is protected, the maximum steel temperature reached in the heating phase of fire can change from a case to another. This is denoted as the initial cooling temperature. The initial cooling temperature can greatly affect the response of the system at the end of the cooling phase. Results of three different initial cooling temperatures (500, 550 and 600°C), following the same heating rate (20°C/min), are presented in Figure 10. It can be clearly seen that as the initial cooling temperature increases, the beam tensile force and mid-span deflection at the end of the cooling phase increase. This is caused by the loss of compressive forces at high temperatures due to creep and catenary action, which results in increased tensile stresses at the cooling phase. As it is assumed that the steel material regains its full strength after cooling, as mentioned before, no failure in the connection is observed.

4.2.5 Beam geometry. In this section, the beam geometry (e.g. size and length) is considered to have more insights on its effect on the creep response. A beam section of UB 305 × 102 × 25 is chosen to replace the existing beam under the same conditions and keeping the same setback distance. The beam length is increased to 4 m with the same applied force (40 kN). This is to maintain the same load ratio (half of the beam ambient plastic moment capacity) without increasing the shear force demand on the connections. The FE results of different heating rates are presented in Figure 11. A higher maximum beam axial force is reached in the heating phase since the beam length and section area are greater than that of the previous beam. Similarly, the beam mid-span deflection is also higher than that of the previous beam. Moreover, for the case of

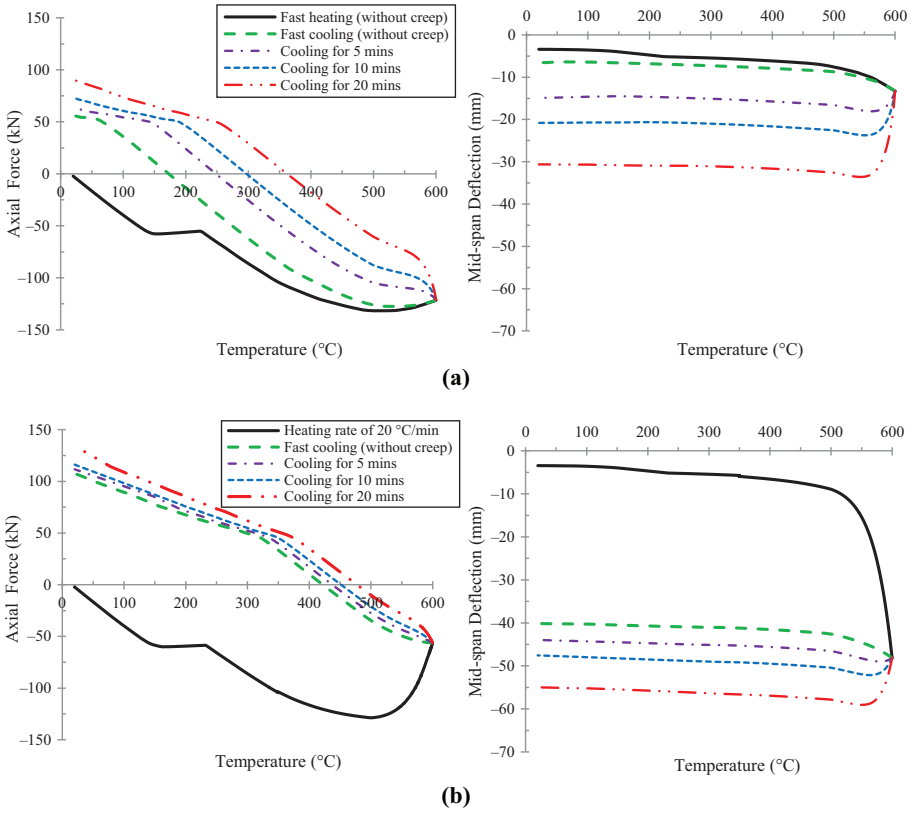

Figure 9. Beam axial force and mid-span deflection response for different cooling durations after: (a) fast heating (without creep) and (b) heating rate of 20° C/min

a slow heating rate (5°C/min), the axial force in the beam changes from compression to tension owing to the high beam deformation. Due to the fact that the setback distance is kept unchanged and the beam depth and length are increased, the beam comes in contact with the column at an earlier stage. Furthermore, lateral torsional buckling of the bottom flange and local buckling of the beam web near the shear tab are observed.

4.2.6 Shear tab location. In the current design practice, the shear tab is typically shifted to the upper portion of the beam web. Three cases are considered to study the effect of the shear tab location on the performance of the frame in fire: 0, 25 and 50 mm above the beam center line. The beam in the previous section (UB 305 × 102 × 25) is used because it allows for more space to move the shear tab away from the beam center line. The results are illustrated in Figure 12. The results show that the location of the shear tab with respect to the beam centerline does not have a significant effect on the results; however, slight changes can be observed. The more the distance between the shear tab plate and the beam centerline increases, the earlier the beam bottom flange comes in contact with the column. This is evident since the contact angle decreases. Shifting the shear tab plate from the beam centerline also results in an increase in the deflection at low temperatures. This can be related to the increase in the P-Δ effect explained previously. However, at late stages of fire, this behavior changes. It is observed that shifting the shear tab plate above the beam center line results in less mid-span deflection and less drop in the axial force. This can be due to the

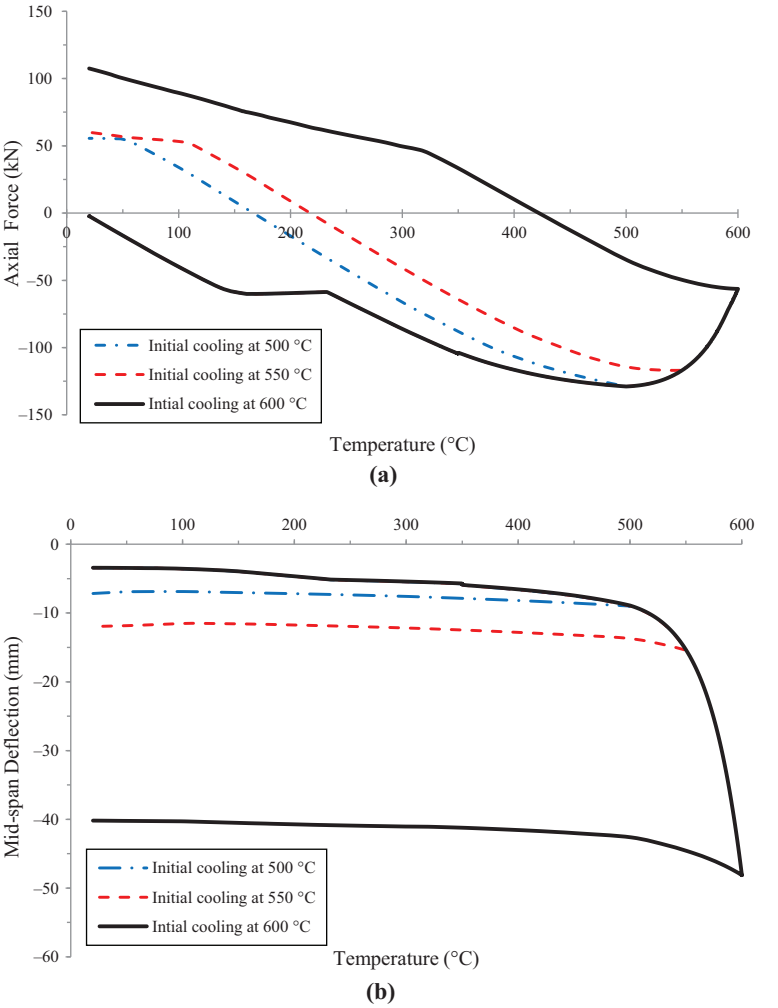

Figure 10.
Results for varying initial cooling temperatures following a heating rate of 20°C/min

Notes: (a) Beam axial force; (b) beam mid-span deflection

additional connection rotational stiffness (increase in the lever arm as the offset distance increases) following the beam-column contact.

5. Conclusions

The purpose of this study was to evaluate the influence of key parameters on the time-dependent behavior of steel frames with shear tab connections in fire. Transient-state conditions were applied in the study which is more representative of building fires than steady-state conditions. Extensive parametric studies were carried out after validating the FE models results against that of experimental work available in the literature. As it is clearly evident from the study, considering time in structural fire analysis is of

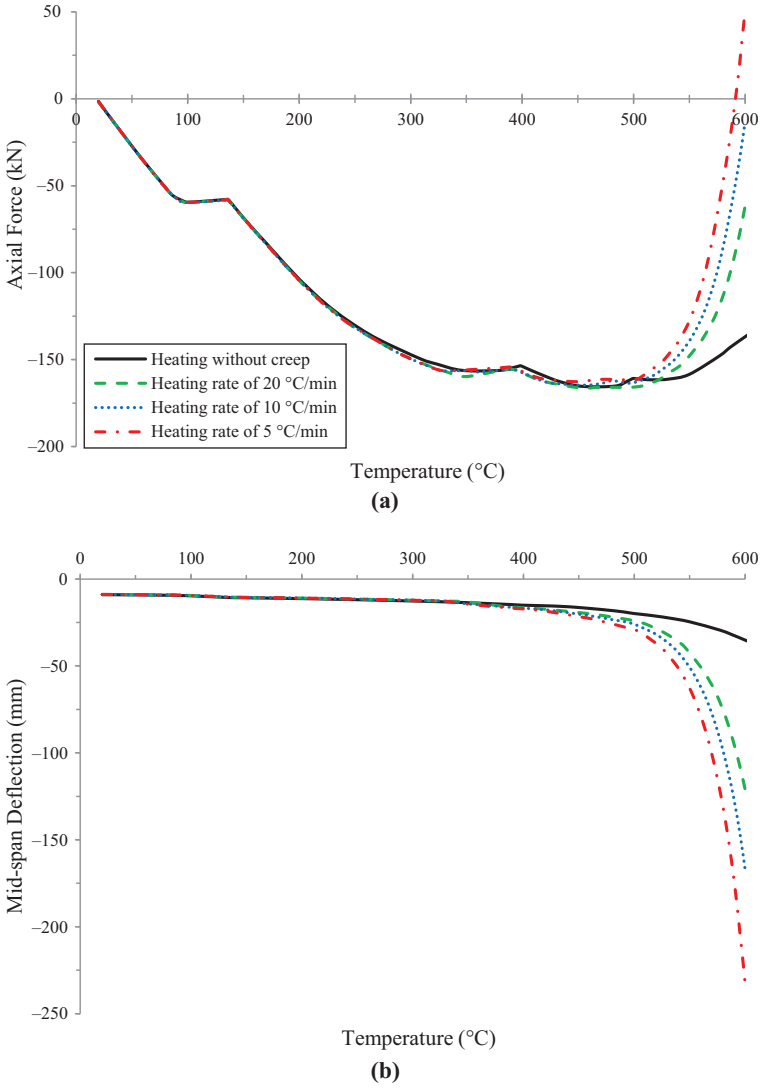

Notes: (a) Beam axial force; (b) beam mid-span deflection

Figure 11.
Results of UB 305 × 102 × 25 beam for different heating rates

great importance especially when reaching high temperatures where creep effect is of high significance. It is worth mentioning that more experimental and numerical studies that focus on the time-dependent behavior of steel structures are still needed. Creep effect should be investigated for temperatures higher than 600°C, and more reliable creep models should be developed to include the creep effect in other structural components (columns, bolts, welds. . .). Further, the effect of the beam thermal gradient and different design fire curves on the structural system should be investigated. The following points can be concluded from this study:

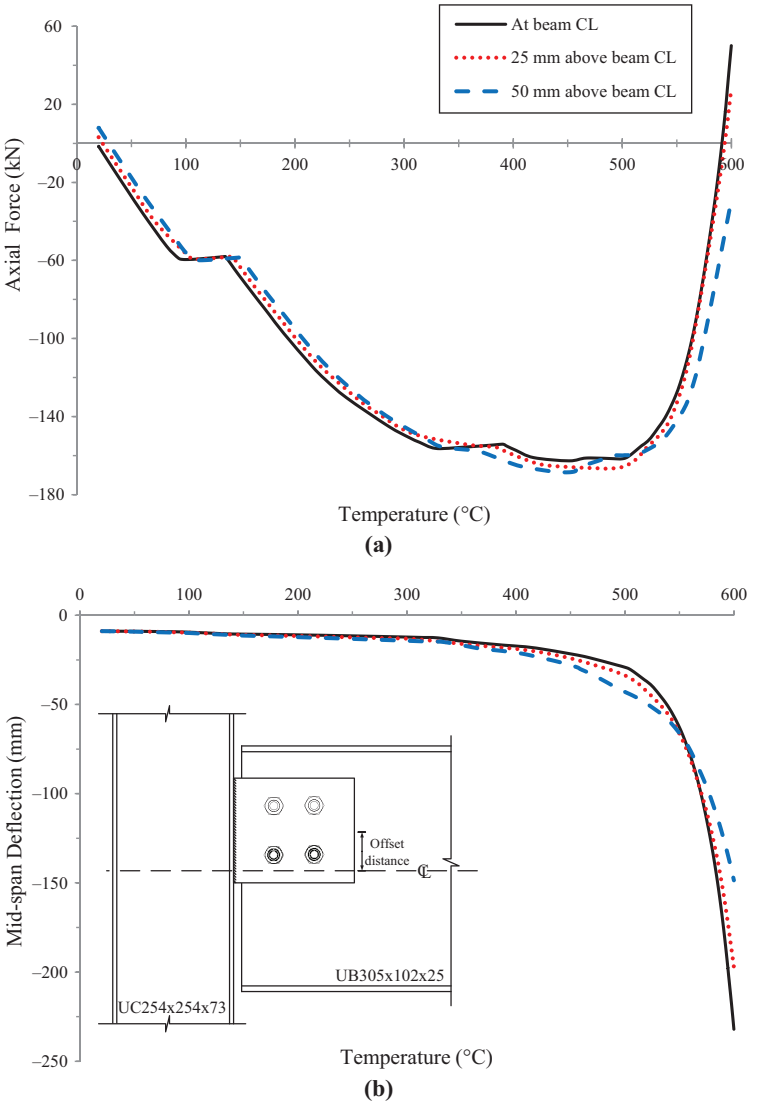

Figure 12.
Results of UB 305 × 102 × 25 beam with different shear tab locations

Notes: (a) Beam axial force; (b) beam mid-span deflection

- The newly developed subroutine has proven to account for various conditions. It can be applied to any FE model in Abaqus under certain conditions and limitations (material, temperature range. . .).
- Slower heating rates reduce the beam axial stresses due to stress relaxation phenomenon, and at the same time increases the beam deflection due to creep effect. For instance, about 80 per cent decrease in the beam axial force and around eight

times increase in the mid-span deflection were observed at the end of slow heating rate (5°C/min), compared to the case with no creep, of Test 1 (Figure 7).

- Two column sizes were used in the study. The FE simulations showed that both columns resulted in relatively similar beam deflection. However, it was shown that the heavier column section can increase the induced axial force in the beam, thus increasing the development of creep strains. As shown in Figure 7, for the case of slow heating (5°C/min) of Test 6, the decrease in the beam axial force was observed to be 30 per cent (compared to the 80 per cent of Test 1), while the midspan deflection shows a similar trend.
- In fire events, the shear tab connection region is subjected to high stresses making the development of creep strain significant at the connection region. This can be observed through the excessive bolt hole ovalization.
- For longer durations (slow heating rate) and under high stress and temperature, creep effect can have a great impact on the structural response and can change the stability configuration of the structure, thus changing the failure mode.
- According to the adopted creep model, by Fields and Fields (1989), the behavior of steel material is highly time-dependent for temperatures above 500°C, where the great impact on steel elements behavior can be observed. Whereas, for temperatures below 400°C, the creep effect is not significant.
- Slower heating rates, higher initial cooling temperatures and longer cooling durations produce higher beam tensile force and larger mid-span deflection at the end of the cooling phase.
- The shear tab location, with respect to the beam centerline has a slight effect on the beam behavior at early stages of fire. However, the results show that as the location of the shear tab moves above the beam centerline, the deflection of the beam reduces due to the increased stiffness (lever arm) of the connection following the beam-column contact.

References

Abaqus Ver. 6.14 Documentation (2014), *Dassault Systemes Simulia Corporation*.

Dwaikat, M. and Kodur, V. (2009), "Effect of location of restraint on fire response of steel beams", *Fire Technology*, Vol. 46 No. 1, pp. 109-128.

EN 1995-1-2 (2005), *Eurocode 3- Design of Steel Structures – Part 1-2: General Rules – Structural Fire Design*, European Committee for Standardization, Brussels.

Fields, B.A. and Fields, R.J. (1989), *Elevated Temperature Deformation of Structural Steel*, National Institute of Standards and Technology (NIST).

Hantouche, E.G. and Sleiman, S.A. (2015), "Isolated shear endplate and double angle connections: prediction of strength capacity", *Structures Congress*, pp. 2153-2163.

Harmathy, T.Z. (1967), "A comprehensive creep model", *Journal of Basic Engineering*, Vol. 89 No. 3, pp. 496-502.

Hu, G. and Engelhardt, M.D. (2014), "Experimental investigation of steel single plate beam end connections at elevated temperatures", *Engineering Structures*, Vol. 58, pp. 141-151.

Hu, Y., Davison, J.B., Burgess, I.W. and Plank, R.J. (2007), "Comparative study of the behaviour of BS 4190 and BS EN ISO 4014 bolts in fire", *3rd, International Conference on Steel and Composite Structures*, *Taylor and Francis*, *Manchester*, pp. 587-592.

Huang, Z.-F. and Tan, K.-H. (2004), "Effects of external bending moments and heating schemes on the responses of thermally restrained steel columns", *Engineering Structures*, Vol. 26 No. 6, pp. 769-780.

Kodur, V. and Dwaikat, M. (2010), "Effect of high temperature creep on the fire response of restrained steel beams", *Materials and Structures*, Vol. 43 No. 10, pp. 1327-1341.

Lee, J., Morovat, M.A., Hu, G., Engelhardt, M.D. and Taleff, E. (2013), "Experimental investigation of mechanical properties of ASTM A992 steel at elevated temperatures", *Eng. J*, Vol. 50 No. 4, pp. 249-272.

Lie, T.T. (1992), *Structural Fire Protection*, ASCE - American Society of Civil Engineers.

Luecke, W.E., McColskey, J.D., McCowan, C.N., Banovic, S.W., Fields, R.J., Foecke, T.J., Siewert, T.A. and Gayle, F.W. (2005), *Federal Building and Fire Safety Investigation of the World Trade Center – Mechanical Properties of Structural Steels, Report NIST NCSTAR 1-3D*, National Institute of Standards and Technology, Gaithersburg, MD.

Matar, M., Rahman, A. and Shrih, A. (2014), "Primary creep in ASTM A325 bolts under simulated fire loading", *Journal of Structural Fire Engineering*, Vol. 6 No. 1, pp. 28-33.

Morovat, M.A., El Ghor, A.H. and Hantouche, E.G. (2018), "Time-Dependent response of flush endplate connections to fire temperatures", *Journal of Structural Engineering*, Vol. 144 No. 4, p. 4018023.

Morovat, M.A., Engelhardt, M.D., Helwig, T. and Taleff, E. (2014), "High-Temperature creep buckling phenomenon of steel columns subjected to fire", *Journal of Structural Fire Engineering*, Vol. 5 No. 3, pp. 189-202.

Pakala, P. and Kodur, V. (2016), "Effect of concrete slab on the behavior of fire exposed subframe assemblies with bolted double angle connections", *Engineering Structures*, Vol. 107, pp. 101-115.

Poh, K.W. (2001), "Stress-strain-temperature relationship for structural steel", *Journal of Materials in Civil Engineering*, Vol. 13 No. 5, pp. 371-379.

Selamet, S. and Garlock, M. (2010), "Robust fire design of single plate shear connections", *Engineering Structures*, Vol. 32 No. 8, pp. 2367-2378.

Tan, K.H., Ting, S.K. and Huang, Z.F. (2002), "Visco-Elasto-Plastic analysis of steel frames in fire", *J. Struct. Eng*, Vol. 128 No. 1, pp. 105-114.

Torić, N., Harapin, A. and Boko, I. (2013), "Experimental verification of a newly developed implicit creep model for steel structures exposed to fire", *Engineering Structures*, Vol. 57, pp. 116-124.

Wald, F.A., Simões da Silva, L.B., Moore, D.B.C., Lennon, T.C., Chladná, M.D., Santiago, A.B., Beneš, M.A. and , Borges, L.B. (2006), "Experimental behaviour of a steel structure under natural fire", *Fire Safety Journal*, Vol. 41 No. 7, pp. 509-522.

Wang, W., Yan, S. and Kodur, V. (2016), "Temperature induced creep in Low-Alloy structural Q345 steel", *Journal of Materials in Civil Engineering*, Vol. 28 No. 6, p. 6016003.

Wang, Y.C., Dai, X.H. and Bailey, C.G. (2011), "An experimental study of relative structural fire behaviour and robustness of different types of steel joint in restrained steel frames", *Journal of Constructional Steel Research*, Vol. 67 No. 7, pp. 1149-1163.

Williams-Leir, G. (1983), "Creep of structural steel in fire: analytical expressions", *Fire and Materials*, Vol. 7 No. 2, pp. 73-78.

Yu, H., Burgess, I.W., Davison, J.B. and Plank, R.J. (2009a), "Tying capacity of web cleat connections in fire, part 1: test and finite element simulation", *Engineering Structures*, Vol. 31 No. 3, pp. 651-663.

Yu, H., Burgess, I.W., Davison, J.B. and Plank, R.J. (2009b), "Experimental investigation of the behaviour of fin plate connections in fire", *Journal of Constructional Steel Research*, Vol. 65 No. 3, pp. 723-736.

Corresponding author
Elie Hantouche can be contacted at: elie.hantouche@aub.edu.lb